Efficient Analytic Technique for Fractional Fourth-Order Cubic Nonlinear Schrodinger Equation

Ahmed Hagag[1], Zuhur Alqahtani[2,*] and Anas Arafa[3,4]

[1] Department of Basic Science, Faculty of Engineering, Sinai University-Kantara Branch, Ismailia, 41636, Egypt

[2] Department of Mathematical Sciences, College of Science, Princess Nourah bint Abdulrahman University, P.O. Box 84428, Riyadh, 11671, Saudi Arabia

[3] Department of Mathematics, College of Sciences and Arts, Qassim University, Al Mithnab, Buraydah, 51452, Saudi Arabia

[4] Department of Mathematics, Faculty of Science, Port Said University, Port Said, 42526, Egypt

INFORMATION

Keywords:
Dispersive cubic fourth-order nonlinear schrodinger equation (DNLS)
optical fiber field
q-homotopy analysis transform method
convergence analysis

DOI: 10.23967/j.rimni.2025.10.60138

SCIPEDIA Revista Internacional de Métodos Numéricos para Cálculo y Diseño en Ingeniería

Revista Internacional Métodos numéricos para cálculo y diseño en ingeniería RIMNI CIMNE

Efficient Analytic Technique for Fractional Fourth-Order Cubic Nonlinear Schrodinger Equation

Ahmed Hagag[1], **Zuhur Alqahtani**[2,*] **and Anas Arafa**[3,4]

[1]Department of Basic Science, Faculty of Engineering, Sinai University-Kantara Branch, Ismailia, 41636, Egypt

[2]Department of Mathematical Sciences, College of Science, Princess Nourah bint Abdulrahman University, P.O. Box 84428, Riyadh, 11671, Saudi Arabia

[3]Department of Mathematics, College of Sciences and Arts, Qassim University, Al Mithnab, Buraydah, 51452, Saudi Arabia

[4]Department of Mathematics, Faculty of Science, Port Said University, Port Said, 42526, Egypt

ABSTRACT

This paper presents an advanced analytical solution for the fractional fourth-order dispersive cubic nonlinear Schrödinger equation (DNLS), a model significant for engineering applications in optical fiber systems, quantum mechanics, and plasma physics. This work leverages the q-homotopy analysis transform method (q-HATM) to address the challenges in modeling complex, nonlinear wave propagation in engineering and physics applications involving fractional dynamics. By providing highly accurate, convergent solutions, this method allows engineers and scientists to model memory effects and higher-order dispersions more effectively in systems like optical waveguides and plasma waves. The demonstrated accuracy and convergence of q-HATM establish it as a practical tool for researchers aiming to solve complex wave propagation problems, advancing both theoretical understanding and real-world engineering solutions in nonlinear optics, quantum fields, and other areas requiring precise modeling of wave interactions.

OPEN ACCESS

Received: 25/10/2024

Accepted: 05/03/2025

Published: 20/04/2025

DOI
10.23967/j.rimni.2025.10.60138

Keywords:
Dispersive cubic fourth-order nonlinear schrodinger equation (DNLS)
optical fiber field
q-homotopy analysis transform method
convergence analysis

1 Introduction

The analytical solutions of nonlinear differential equations (NLDEs) have proven important in the past few decades because they seem to be the foundation of the mathematical models of intricate physical problems in many different frameworks, including mechanics, physics, chemistry, biology, and engineering.

Numerical methods, especially those that accurately solve fractional-order equations, play an essential role in engineering, where modeling complex systems with memory and nonlinearity is

*Correspondence: Zuhur Alqahtani (zumalqahtani@pnu.edu.sa).

critical. In fields like optical communications and plasma physics, the accurate prediction of wave propagation, stability, and dispersion is fundamental to both design and innovation. By providing a framework to manage fractional dynamics, q-HATM allows engineers to simulate complex behaviors in these systems, resulting in better performance predictions and enabling advancements in technologies reliant on high-precision modeling.

Several analytical and numerical methods have been developed to solve both linear and nonlinear partial differential equations, including the differential transform method (DTM) [1,2], the perturbation methods (PM) [3,4], the Adams Bashforth Moulton method (ABMM) [5], the Laplace decomposition method (LDM) [6,7], the variational method (VM) [8,9], the He's polynomial method (HPM) [10,11], the Temimi Ansari method [12,13], the natural decomposition method [14] and others [15–17]. Among these methods, the homotopy analysis transform method (HATM) has proven particularly effective due to its flexibility in controlling convergence. The HATM, as demonstrated in [18], has been successfully applied to solve a wide range of linear and nonlinear problems. In [19], the q-HATM (a modification of HATM) was introduced to improve convergence and accuracy in fractional differential equations. This method incorporates an auxiliary parameter λ to regulate the region of convergence, making it a valuable tool for complex systems with memory effects, as outlined in [20]. The application of q-HATM to fractional partial differential equations has also been explored in [21], where the method was shown to provide highly accurate solutions for fractional-order systems with higher-order dispersions. By leveraging the fractional framework, q-HATM effectively models systems with hereditary effects, overcoming limitations seen in classical approaches like HPM and LDM. This flexibility makes q-HATM particularly well-suited for addressing higher-order dispersive effects and nonlinearities.

The HATM is an approximation method that has been used extensively in solving linear and nonlinear equations with applications in engineering, finance, economics, fundamental science, and applied mathematics. This approach is superior to all other approximation methods due to the inclusion of parameter λ, which regulates the region of convergence and enhances the accuracy of the method. It is already recognized that Schrodinger's nonlinear (NLS) equation is broadly utilized in numerous fields of physics in the basic models of nonlinear waves [22]. It arises from the study of the proliferation of nonlinear waves in inhomogeneous and dispersive media, for example, nonuniform dielectric media and plasma phenomena [23–25].

The derivative cubic nonlinear Schrodinger equation (DNLS) is a dispersive model that appears in the plasma, especially in the wave propagation description. Since Schrodinger's nonlinear derivative equation is one of the important integrable models, it has many vital and varied applications of chemical, biological, and physical phenomena. and the DNLS equation is sometimes present in the form of different nonlinear waves, it emerges in many fields of applied mathematics and many branches of physics, such as femtosecond or sub-picosecond pulses in optical fibers [26], nonlinear Alfven waves [27], weak nonlinear electromagnetic waves, condensed matter physics, and quantum field theory [28].

We can write the following fractional dispersive cubic nonlinear Schrodinger equation (DNLS) of the fourth order as

$$i\frac{\partial^{\alpha} v}{\partial t^{\alpha}} + a\frac{\partial^{2} v}{\partial x^{2}} - b\frac{\partial^{4} v}{\partial x^{4}} + c|v|^{2}v = 0, 0 < \alpha \leq 1, \tag{1}$$

and the fractional nonlinear Schrodinger equation (NLSE) with dual-power law nonlinearity of fourth order as

$$i\frac{\partial^{\alpha} v}{\partial t^{\alpha}} + a\frac{\partial^{2} v}{\partial x^{2}} - b\frac{\partial^{4} v}{\partial x^{4}} + c\left(v + |v|^{2}\right) = 0, \tag{2}$$

this equation is a generalized form of the nonlinear Schrödinger equation (NLS), a fundamental model in the study of wave propagation in nonlinear and dispersive media. The NLS has been extensively used in various fields such as quantum mechanics, nonlinear optics, plasma physics, and condensed matter physics [29–31]. Foundational works such as Ablowitz et al. (1981) have laid the groundwork for understanding soliton dynamics, while more recent studies, including Chabchoub et al. (2015), explore the nonlinear Schrödinger equation in the context of optical fibers and weakly nonlinear wave propagation [32].

The introduction of fractional derivatives in the equation allows for the modeling of systems with memory and hereditary properties, which are important in describing complex physical processes more accurately. Fractional derivatives offer a significant advantage by capturing memory and hereditary effects, enabling more comprehensive and accurate modeling of complex physical systems such as those observed in optical and plasma physics. Furthermore, the fractional framework extends the traditional models to address non-local and history-dependent effects, which are essential for understanding higher-order dispersive and nonlinear dynamics.

Historically, the NLS equation has been used to describe soliton dynamics in optical fibers, wave propagation in plasmas, and many other phenomena involving nonlinear wave interactions. The DNLS, a variant of the NLS, is particularly important in plasma physics and nonlinear optics, where it describes phenomena like nonlinear wave propagation in inhomogeneous media [33–35]. The fourth-order terms in the equation account for higher-order dispersive effects, which are significant in media where such effects cannot be neglected [36,37]. Recent advancements, such as that by Babin et al.(2005), highlight the importance of fractional and nonlinear modeling in addressing challenges in wave dynamics and optical solitons [24].

The motivation for studying this particular form of the DNLS stems from the need to understand complex wave dynamics in modern optical and quantum systems. With advancements in technology, such as the development of ultra-fast and ultra-short optical pulses, higher-order effects and fractional dynamics become increasingly relevant. The fractional order model provides a more comprehensive framework for capturing the subtleties of wave propagation and interaction in these advanced systems.

Furthermore, the study aims to enhance analytical techniques for solving such complex equations. The q-Homotopy Analysis Transform Method (q-HATM) is explored as a powerful tool for obtaining approximate solutions to the fractional DNLS equation. By comparing these solutions with exact solutions, the study not only validates the effectiveness of q-HATM but also contributes to the broader understanding of fractional differential equations in modeling real-world physical systems.

In summary, the historical importance of the DNLS equation in modeling nonlinear wave phenomena, combined with the modern need for accurate models incorporating memory effects, drives the current research. This study addresses these challenges by employing fractional calculus and advanced analytical techniques, thus contributing to both theoretical knowledge and practical applications in physics and engineering.

The remainder of this paper is organized as follows: Section 2 provides the necessary preliminary information, introducing the fundamental concepts of fractional calculus that underpin our approach. In Section 3, we detail the formulation of the q-HATM as applied to the fractional fourth-order cubic nonlinear Schrödinger equation. In Section 4, we discuss numerical results and provide comprehensive comparisons between the q-HATM and other existing methods, showcasing the accuracy and efficiency of our approach. Section 5 wraps up the work by highlighting the main conclusions and outlining possible avenues for further investigation.

2 Preliminaries

This portion will provide enough information to recognize the fractional calculus theory. The term fractional calculus has been defined in a variety of ways over the past 200 years. These definitions include Hadamard fractional derivative, Grünwald-Letnikov fractional derivative, Marchaud fractional derivative, Riesz fractional derivative, and Caputo fractional derivative.

Definition 1: *The Riemann-Liouville fractional integral operator of a functional* $g \in C_\mu, \mu \geq -1$ *is denoted by* J_b^α *and defined as [38]*

$$J_b^\alpha g(y) = \frac{1}{\Gamma(\alpha)} \int_b^y (y-\zeta)^{\alpha-1} g(\zeta) d\zeta, y, \alpha > 0. \tag{3}$$

For $g \in C_\mu^m, \beta, \alpha > 0, \gamma \geq -1$ *and* $\mu \geq -1$, *we can remember the next properties of the operator* J_b^α *[39].*

1. $J_b^\alpha g(y)$ *exist for almost every* $y \in [b, d]$,
2. $J_b^\alpha J_b^\beta g(y) = J_b^{\alpha+\beta} g(y)$,
3. $J_b^\alpha J_b^\beta g(y) = J_b^\beta J_b^\alpha g(y)$,
4. $J_b^\alpha (y-b)^\gamma = \dfrac{\Gamma(\gamma+1)}{\Gamma(\alpha+\gamma+1)} (y-b)^{\alpha+\gamma}$.

Definition 2: *We can write Laplace transform (LT) for any function* $v(t)$ *if* $n \in N$ *as*

$$\ell \left\{ \frac{d^r}{dx^r}; v; s \right\} = s^r V(s) - \sum_l^{r-1} s^{r-l-1} v^{(l)} \left(0^+\right), \tag{4}$$

then, using the LT, the Caputo fractional derivative is obtained as follows [38]:

$$\ell \left\{ D_t^\alpha v \right\} = s^\alpha \ell\{v\} - \sum_l^{r-1} s^{\alpha-l-1} v^{(l)} \left(0^+\right), r-1 < \alpha \leq r. \tag{5}$$

3 Formulation of q-HATM

Here, a quick and detailed discussion of the q-HATM will be provided; refer to [19–21]. Let's look at the following nonlinear fractional differential equation:

$$D_t^\alpha v(y,z) + Rv(y,z) + Nv(y,z) = w(y,z), r-1 < \alpha \leq r, \tag{6}$$

where $D_t^\alpha = \dfrac{\partial^\alpha}{\partial t^\alpha}$ is the Caputo fractional derivative, R denotes the linear operator, N indicates to the nonlinear differential operator and $g(y,z)$ denotes the continuous functions. Using the LT to modify the two sides of Eq. (6), we get

$$\ell \left\{ D_t^\alpha v(y,z) \right\} + \ell \{Rv(y,z)\} + \ell \{Nv(y,z)\} = \ell \{w(y,z)\}. \tag{7}$$

Applying LT to Eq. (7), we get

$$s^\alpha \ell \{v\} - \sum_l^{r-1} s^{\alpha-l-1} v^{(l)}(y,0) + \ell \{Rv\} + \ell \{Nv\} = \ell \{w(y,z)\}. \tag{8}$$

where $\ell \left\{ D_t^\alpha v(y,z) \right\} = s^\alpha \ell\{v\} - \sum_l^{r-1} s^{\alpha-l-1} v^{(l)}(y,0)$. At this point, the definition of a non-linear operator may be found here:

$$N[\Upsilon(y,z;q)] = \ell \{\Upsilon(y,z;q)\} - \frac{f(y)}{s} - \frac{h(y)}{s^2} + \frac{1}{s^\alpha} \ell \{R\mathrm{r}(y,z;q)\} + \frac{1}{s^\alpha} \ell \{N\Upsilon(y,z;q)\} - \frac{1}{s^\alpha} \ell \{w(y,z)\}, \tag{9}$$

where $q \in \left[0, \frac{1}{n}\right]$, and $\Upsilon(y,z;q)$ denotes the real function of y, z and q. We may use the following to show how the homotopy approach was created:

$$[1-nq]\,L\left[\mathrm{r}\left(y,z;q\right)-v_0\left(y,0\right)\right]=\lambda q H\left(y,z\right)N\left[v\left(y,z\right)\right], \tag{10}$$

where $\lambda \neq 0$ is an accessory parameter, $v_0(y,0)$ is an initial condition of $v(y,z)$, $\mathrm{r}(y,z;q)$ is an obscure function and $H(y,z) \neq 0$ is depicting a nonzero accessory function. Amplification $\Upsilon(y,z;q)$ with respect to q and using Taylor series, we get

$$\Upsilon\left(y,z,q\right)=v_0\left(y,z\right)+\sum\nolimits_{m=1}^{\infty} v_m\left(y,z\right)q^m, \tag{11}$$

where

$$v_m\left(y,z\right)=\frac{1}{m!}\frac{\partial^m \Upsilon\left(y,z,q\right)}{\partial q^m}\bigg|_{q=0}. \tag{12}$$

Suppose that at $q \to \frac{1}{n}$, the choices of $\lambda, L, H(y,z)$, and $v_0(y,0)$ cause the series (11) to converge, then

$$v\left(y,z\right)=v_0\left(y,z\right)+\sum\nolimits_{m=1}^{\infty} v_m\left(y,z\right)\left(\frac{1}{n}\right)^m. \tag{13}$$

By differentiation Eq. (10) with respect to q by m times then dividing by m! and put q = 0, we get

$$\ell\left\{v_m(y,z)-\chi_m v_{m-1}(y,z)\right\}=\lambda H\left(y,z\right)R_m\left(\vec{v}_{m-1}\right). \tag{14}$$

Applying the inverse Laplace transform to modify both sides of Eq. (14) yields

$$v_m\left(y,z\right)=\chi_m v_{m-1}\left(y,z\right)+\lambda H\left(y,z\right)\ell^{-1}\left\{R_m\left(\vec{v}_{m-1}\right)\right\}, \tag{15}$$

where in $R_m\left(\vec{v}_{m-1}\right)$ is shown as

$$R_m\left(\vec{v}_{m-1}\right)=\frac{1}{(m-1)!}\frac{\partial^{m-1}N[\Upsilon(y,z,q)]}{\partial q^{m-1}}\bigg|_{q=0}, \tag{16}$$

where $\chi_m=\begin{cases}0, & m\leq 1,\\ n, & m>1\end{cases}$. Finally, we get $v(y,z)=\sum_{m=0}^{N} v_m(y,z)\left(\frac{1}{n}\right)^m$.

4 Numerical Results

This section deals with the fractional dispersive cubic nonlinear Schrodinger equation (DNLS) of the fourth order as

$$i\frac{\partial^\alpha v}{\partial t^\alpha}+a\frac{\partial^2 v}{\partial x^2}-b\frac{\partial^4 v}{\partial x^4}+c|v|^2 v=0, 0<\alpha\leq 1, \tag{17}$$

with four initial conditions and four exact solutions as [40] $\begin{cases}v(x,0)=f(x)\\ v(x,t)=F(x,t)\end{cases}$, $v = v(x,t)$ is a complex valued function. If $b = 0$, Eq. (1) converts to standard second order (NLS) equation.

We can write the following fractional nonlinear Schrodinger equation of the fourth order which takes the operator form as

$$D_t^{\alpha} v(x,t) = i\left[a v_{2x} - b v_{4x} + c v^2 v^*\right]. \tag{18}$$

Regarding the q-HATM, the Laplace operator and the general operator may be defined as

$$N\left[\Upsilon(x,t;q)\right] = \ell\left\{\Upsilon(x,t;q)\right\} - \left(1-\frac{\chi_m}{n}\right)\frac{f(x)}{s} - \frac{i}{s^{\alpha}}\ell\Big\{a(\Upsilon(x,t;q))_{2x} - b(\Upsilon(x,t;q))_{4x} + c\Upsilon^2(x,t;q)\overset{*}{\Upsilon}(x,t;q)\Big\}, \tag{19}$$

$$\ell\left\{v_m(x,t) - \chi_m v_{m-1}(x,t)\right\} = \lambda R_m\left(\vec{v}_{m-1}\right), \tag{20}$$

respectively, where

$$R_m\left(\vec{v}_{m-1}\right) = \ell\left\{v_{m-1}\right\} - \left(1-\frac{\chi_m}{n}\right)\left(\frac{f(x)}{s}\right) - \frac{i}{s^{\alpha}}\ell\left\{a\left(v_{m-1}\right)_{2x} - b\left(v_{m-1}\right)_{4x} + c\sum_{i=0}^{m-1}\sum_{j=0}^{i} v_j v_{i-j} v^*_{m-1-i}\right\}. \tag{21}$$

It is clear that the solution of the Eq. (20) for $m \geq 1$ become

$$\begin{aligned} v_m(x,t) &= \chi_m v_{m-1} + \lambda\ell^{-1}\left\{R_m\left(\vec{v}_{m-1}\right)\right\}, \\ v_m(x,t) &= \left(\chi_m+\lambda\right)v_{m-1} - \lambda\left(1-\frac{\chi_m}{n}\right)\ell^{-1}\left\{\frac{f(x)}{s}\right\} - \lambda\ell^{-1}\left\{\left(\frac{i}{s^{\alpha}}\right)\ell\left\{a\left(v_{m-1}\right)_{2x} - b\left(v_{m-1}\right)_{4x}\right.\right. \\ &\quad \left.\left. + c\sum_{i=0}^{m-1}\sum_{j=0}^{i} v_j v_{i-j} v^*_{m-1-i}\right\}\right\} \end{aligned} \tag{22}$$

Through solving the above equation with $f(x) = v(x,0)$, that we can get $v(x,t) = \sum_{m=0}^{N} v_m\left(\frac{1}{n}\right)^m$.

4.1 Application 1

The first periodic solution and initial condition for Eq. (1) may be expressed as follows:

$$\begin{cases} v(x,t) = \sqrt{\dfrac{3a^2}{10bc}}\sec^2\left(x\sqrt{\dfrac{-a}{20b}}\right)\exp\left(\dfrac{4ia^2t}{25b}\right), & \dfrac{a}{b} < 0, \\ v(x,0) = \sqrt{\dfrac{3a^2}{10bc}}\sec^2\left(x\sqrt{\dfrac{-a}{20b}}\right) \end{cases}. \tag{23}$$

On solving Eq. (22) by using q-HATM, we get

$$v(x,t) = \sqrt{\frac{3a^2}{10bc}}\sec^2\left(x\sqrt{\frac{-a}{20b}}\right) + \left\{-\frac{2i\sqrt{\frac{6}{5}}c\lambda t^{\alpha}\left(\frac{a^2}{bc}\right)^{3/2}\operatorname{sech}^2\left(\frac{\sqrt{ax}}{2\sqrt{5b}}\right)}{25\Gamma(\alpha+1)}\right\}\left(\frac{1}{n}\right) - \left\{\frac{2\sqrt{\frac{6}{5}}c\lambda t^{\alpha}\left(\frac{a^2}{bc}\right)^{3/2}\operatorname{sech}^2\left(\frac{\sqrt{ax}}{2\sqrt{5b}}\right)\left(4a^2\lambda\Gamma(\alpha+1)t^{\alpha}+25ib\Gamma(2\alpha+1)(n+\lambda)\right)}{625b\Gamma(\alpha+1)\Gamma(2\alpha+1)}\right\}\left(\frac{1}{n}\right)^2+\cdots . \quad (24)$$

4.2 Application 2

The second periodic solution and initial condition for Eq. (1) may be expressed as follows:

$$\begin{cases} v(x,t) = \sqrt{\frac{3a^2}{10bc}}\csc^2\left(x\sqrt{\frac{-a}{20b}}\right)\exp\left(\frac{4ia^2t}{25b}\right), \quad \frac{a}{b}<0, \\ v(x,0) = \sqrt{\frac{3a^2}{10bc}}\csc^2\left(x\sqrt{\frac{-a}{20b}}\right) \end{cases} . \quad (25)$$

On solving Eq. (22) by using q-HATM, we get

$$v(x,t) = \sqrt{\frac{3a^2}{10bc}}\csc^2\left(x\sqrt{\frac{-a}{20b}}\right) + \left\{\frac{2i\sqrt{\frac{6}{5}}c\lambda t^{\alpha}\left(\frac{a^2}{bc}\right)^{3/2}\operatorname{csch}^2\left(\frac{\sqrt{ax}}{2\sqrt{5b}}\right)}{25\Gamma(\alpha+1)}\right\}\left(\frac{1}{n}\right) + \left\{\frac{2\sqrt{\frac{6}{5}}c\lambda t^{\alpha}\left(\frac{a^2}{bc}\right)^{3/2}\operatorname{csch}^2\left(\frac{\sqrt{ax}}{2\sqrt{5b}}\right)\left(4a^2\lambda\Gamma(\alpha+1)t^{\alpha}+25ib\Gamma(2\alpha+1)(n+\lambda)\right)}{625b\Gamma(\alpha+1)\Gamma(2\alpha+1)}\right\}\left(\frac{1}{n}\right)^2+\cdots . \quad (26)$$

4.3 Application 3

The first hyper periodic solution and initial condition for Eq. (1) may be expressed as follows:

$$\begin{cases} v(x,t) = \sqrt{\frac{3a^2}{10bc}}\operatorname{sech}^2\left(x\sqrt{\frac{-a}{20b}}\right)\exp\left(\frac{4ia^2t}{25b}\right), \quad \frac{a}{b}>0, \\ v(x,0) = \sqrt{\frac{3a^2}{10bc}}\operatorname{sech}^2\left(x\sqrt{\frac{-a}{20b}}\right) \end{cases} . \quad (27)$$

On solving Eq. (22) by using q-HATM, we get

$$v(x,t) = \sqrt{\frac{3a^2}{10bc}}\operatorname{sech}^2\left(x\sqrt{\frac{-a}{20b}}\right) + \left\{\frac{3i\sqrt{\frac{3}{10}}c\lambda t^{\alpha}\left(\frac{a^2}{bc}\right)^{3/2}\left(\cos\left(\frac{\sqrt{ax}}{\sqrt{5b}}\right)-4\right)\sec^4\left(\frac{\sqrt{ax}}{2\sqrt{5b}}\right)}{25\Gamma(\alpha+1)}\right\}\left(\frac{1}{n}\right)$$
$$+\left\{\frac{3\sqrt{\frac{3}{10}}c\lambda t^{\alpha}\left(\frac{a^2}{bc}\right)^{3/2}\sec^4\left(\frac{\sqrt{ax}}{2\sqrt{5b}}\right)}{5000b}\left(\frac{200ib(n+\lambda)\left(\cos\left(\frac{\sqrt{ax}}{\sqrt{5b}}\right)-4\right)}{\Gamma(\alpha+1)}-\left(\frac{1}{\Gamma(2\alpha+1)}\right)\right.\right.$$
$$\left.\left.\times\, 3a^2\lambda t^{\alpha}\left(335\cos\left(\frac{\sqrt{ax}}{\sqrt{5b}}\right)-64\cos\left(\frac{2\sqrt{ax}}{\sqrt{5b}}\right)+\cos\left(\frac{3\sqrt{ax}}{\sqrt{5b}}\right)-200\right)\sec^4\left(\frac{\sqrt{ax}}{2\sqrt{5b}}\right)\right)\right\}\left(\frac{1}{n}\right)^2+\cdots \tag{28}$$

4.4 Application 4

The second hyper periodic solution and initial condition for Eq. (1) may be expressed as follows:

$$\begin{cases} v(x,t) = \sqrt{\frac{3a^2}{10bc}}\operatorname{csch}^2\left(x\sqrt{\frac{-a}{20b}}\right)\exp\left(\frac{4ia^2t}{25b}\right), \quad \frac{a}{b}>0, \\ v(x,0) = \sqrt{\frac{3a^2}{10bc}}\operatorname{csch}^2\left(x\sqrt{\frac{-a}{20b}}\right) \end{cases} . \tag{29}$$

On solving Eq. (22) by using q-HATM, we get

$$v(x,t) = \sqrt{\frac{3a^2}{10bc}}\operatorname{csch}^2\left(x\sqrt{\frac{-a}{20b}}\right) + \left\{\frac{3i\sqrt{\frac{3}{10}}c\lambda t^{\alpha}\left(\frac{a^2}{bc}\right)^{3/2}\left(\cos\left(\frac{\sqrt{ax}}{\sqrt{5b}}\right)+4\right)\csc^4\left(\frac{\sqrt{ax}}{2\sqrt{5b}}\right)}{25\Gamma(\alpha+1)}\right\}\left(\frac{1}{n}\right)$$
$$+\left\{\frac{3\sqrt{\frac{3}{10}}c\lambda t^{\alpha}\left(\frac{a^2}{bc}\right)^{3/2}\csc^4\left(\frac{\sqrt{ax}}{2\sqrt{5b}}\right)}{5000b}\left(\frac{200ib(n+\lambda)\left(\cos\left(\frac{\sqrt{ax}}{\sqrt{5b}}\right)+4\right)}{\Gamma(\alpha+1)}-\left(\frac{1}{\Gamma(2\alpha+1)}\right)\right.\right.$$
$$\left.\left.\times,\, 3a^2\lambda t^{\alpha}\left(335\cos\left(\frac{\sqrt{ax}}{\sqrt{5b}}\right)+64\cos\left(\frac{2\sqrt{ax}}{\sqrt{5b}}\right)+\cos\left(\frac{3\sqrt{ax}}{\sqrt{5b}}\right)+200\right)\csc^4\left(\frac{\sqrt{ax}}{2\sqrt{5b}}\right)\right)\right\}\left(\frac{1}{n}\right)^2+\cdots \tag{30}$$

4.5 Application 5

This section deals with the fractional dispersive cubic nonlinear Schrodinger equation (DNLS) of the fourth order as

$$i\frac{\partial^{\alpha}v}{\partial t^{\alpha}} + a\frac{\partial^2 v}{\partial x^2} - b\frac{\partial^4 v}{\partial x^4} + c\left(|v| + |v|^2\right) = 0, 0 < \alpha \leq 1, \tag{31}$$

with four initial conditions and exact solutions as [41] $\begin{cases} v(x,0) = \left(a_0 + \dfrac{2a_0}{e^{\mu x} - 1}\right) e^{i(-kx+\theta)} \\ v(x,t) = \left(a_0 + \dfrac{2a_0}{e^{\mu(x-wt)} - 1}\right) e^{i(-kx+\beta t+\theta)} \end{cases}$.

We can write the following fractional nonlinear Schrodinger equation of the fourth-order which takes the operator form as

$$D_t^{\alpha} v(x,t) = i\left[a v_{2x} - b v_{4x} + c\left(v + v v^*\right)\right]. \tag{32}$$

On solving Eq. (22) by using q-HATM, we get

$$\begin{aligned} v(x,t) = v_0 - \frac{i e^{-2ix} t^{\alpha}}{(e^x - 1)^5 \Gamma(\alpha+1)} \{ & -e^{2ix} + e^{(1+2i)x} + 2e^{(2+2i)x} - 2e^{(3+2i)x} - e^{(4+2i)x} + e^{(5+2i)x} - 11e^{i} \\ & + (77 - 40i)e^{x+i} + (77 + 40i)e^{4x+i} - (90 - 216i)e^{2x+i} - (90 + 216i)e^{3x+i} - 11e^{5x+i} \} \left(\frac{1}{n}\right). \end{aligned} \tag{33}$$

5 Discussion

The key innovation of our work lies in the application of q-HATM, which provides flexible control over the convergence of the solution series using the auxiliary parameter λ. This allows us to achieve highly accurate approximations of the fractional DNLS, addressing limitations in prior methods such as slow convergence or instability in fractional systems with higher-order nonlinearities. Unlike the HPM, which struggles with controlling convergence in fractional systems, q-HATM offers a more robust solution framework for handling fractional derivatives and higher-order dispersion terms, as evidenced by our detailed convergence analysis and numerical results. To validate the effectiveness of the q-HATM, we compare our solutions to exact results obtained from earlier studies by Wazwaz [40,41] and others. Tables 1–5 below show the comparison between the q-HATM solutions and the exact solutions for specific cases of the fractional DNLS. The absolute errors between the approximate and exact solutions are provided to demonstrate the high accuracy of q-HATM.

Table 1: Comparison of 3rd order q-HATM and HAM for (case 1) when t = 1, $n = 1$, a = −1, λ = −1, b = 10, and c = 1 where $E1 = ||v_{Exact}| - |v_{HATM}||$ and $E2 = ||v_{Exact}| - |v_{HAM}||$

x	$\lvert v_{\text{Exact}}\rvert$	$\lvert v_{\text{HATM}}\rvert$	E_1	$\lvert v_{\text{HAM}}\rvert$	E_2	$\alpha = 0.95$	$\alpha = 0.90$
−5	0.19679	0.19679	1.6121E − 9	0.19055	6.24628E − 3	0.196795	0.196793
−4	0.18783	0.18783	1.5387E − 9	0.18187	5.96185E − 3	0.187834	0.187832
−3	0.18123	0.18123	1.4847E − 9	0.17548	5.75249E − 3	0.181238	0.181236
−2	0.17671	0.17671	1.4476E − 9	0.17110	5.60892E − 3	0.176714	0.176713
−1	0.17407	0.17407	1.4260E − 9	0.16854	5.52507E − 3	0.174072	0.174070
0	0.17320	0.17320	1.4188E − 9	0.16770	5.49749E − 3	0.173203	0.173202
1	0.17407	0.17407	1.4260E − 9	0.16854	5.52507E − 3	0.174072	0.174070
2	0.17671	0.17671	1.4476E − 9	0.17110	5.60892E − 3	0.176714	0.176713
3	0.18123	0.18123	1.4847E − 9	0.17548	5.75249E − 3	0.181238	0.181236
4	0.18783	0.18783	1.5387E − 9	0.18187	5.96185E − 3	0.187834	0.187832
5	0.19679	0.19679	1.6121E − 9	0.19055	6.24628E − 3	0.196795	0.196793

Table 2: Comparison of q-HATM and HAM for (case 2) when $\lambda = -1$, a $= -1$, b $= 10$, and c $= 1$

x	$\lvert v_{\text{Eaxt}} \rvert$	$\lvert v_{\text{HATM}} \rvert$	E_1	$\lvert v_{\text{HAM}} \rvert$	E_2	$\alpha = 0.95$	$\alpha = 0.90$
−5	1.44484	1.44484	1.1836E − 8	1.44438	4.59944E − 4	1.444838	1.444827
−4	2.22373	2.22373	1.8216E − 8	2.22303	7.02857E − 4	2.223719	2.223702
−3	3.90726	3.90726	3.2008E − 8	3.90605	1.20302E − 3	3.907233	3.907204
−2	8.71822	8.71822	7.1419E − 8	8.71595	2.26490E − 3	8.718161	8.718095
−1	34.6988	34.6988	2.8425E − 7	34.7207	2.19847E − 2	34.69857	34.69831
1	34.6988	34.6988	2.8425E − 7	34.7207	2.19847E − 2	34.69857	34.69831
2	8.71822	8.71822	7.1419E − 8	8.71595	2.26490E − 3	8.718161	8.718095
3	3.90726	3.90726	3.2008E − 8	3.90605	1.20302E − 3	3.907233	3.907204
4	2.22373	2.22373	1.8216E − 8	2.22303	7.02857E − 4	2.223719	2.223702
5	1.44484	1.44484	1.1836E − 8	1.44438	4.59944E − 4	1.444838	1.444827

Table 3: Comparison of q-HATM and HAM for (case 3) when $\lambda = -0.1$, a $= 1$, b $= 10$, and c $= 1$

x	$\lvert v_{\text{Exact}} \rvert$	$\lvert v_{\text{HATM}} \rvert$	E_1	$\lvert v_{\text{HAM}} \rvert$	E_2	$\alpha = 0.95$	$\alpha = 0.90$
−5	0.19679	0.19680	5.7831E − 6	0.19527	1.5215E − 3	0.196802	0.196802
−4	0.18783	0.18783	4.5224E − 6	0.18651	1.3232E − 3	0.187840	0.187840
−3	0.18123	0.18124	3.7378E − 6	0.18005	1.1887E − 3	0.181243	0.181243
−2	0.17671	0.17671	3.2638E − 6	0.17561	1.1020E − 3	0.176719	0.176719
−1	0.17407	0.17407	3.0095E − 6	0.17302	1.0534E − 3	0.174077	0.174077
0	0.17320	0.17320	2.9293E − 6	0.17216	1.0377E − 3	0.173208	0.173208
1	0.17407	0.17407	3.0095E − 6	0.17302	1.0534E − 3	0.174077	0.174077
2	0.17671	0.17671	3.2638E − 6	0.17561	1.1020E − 3	0.176719	0.176719
3	0.18123	0.18124	3.7378E − 6	0.18005	1.1887E − 3	0.181243	0.181243
4	0.18783	0.18783	4.5224E − 6	0.18651	1.3232E − 3	0.187840	0.187840
5	0.19679	0.19680	5.7831E − 6	0.19527	1.5215E − 3	0.196802	0.196802

The figures in this paper illustrate the accuracy and effectiveness of the q-HATM in approximating solutions to the fractional fourth-order cubic nonlinear Schrödinger equation (DNLS). The plots and tables compare the q-HATM results with exact solutions and other existing methods, showcasing the performance of q-HATM under different conditions. Fig. 1a,b shows the exact solution and the q-HATM approximation for the third-order DNLS solution for case 1 at parameters $\lambda = -1, \alpha = 1$, $n = 1$, $a = -1$, $b = 10$, and $c = 1$. The close agreement between the exact and q-HATM approximate solutions demonstrates the high accuracy of q-HATM in capturing the nonlinear wave dynamics of the system. The minor discrepancies between the two solutions, as shown in the error metrics, are minimal, indicating the method's reliability. Fig. 2a,b depicts the influence of the auxiliary parameter λ on the accuracy of the solution. The λ-curve highlights how changes in λ impact convergence at specific points, such as $x = 1$, confirming that optimal control over convergence is possible. Similarly, the α-curve illustrates the behavior of the solution across different fractional orders of α, emphasizing the versatility of the q-HATM in handling fractional dynamics.

Table 4: Comparison of q-HATM and HAM for (case 4) when $\lambda = -0.001$, a = 1, b = 10, and c = 1

x	$\lvert v_{\text{Euct}} \rvert$	$\lvert v_{\text{HATM}} \rvert$	E_1	$\lvert v_{\text{HAM}} \rvert$	E_2	$\alpha = 0.95$	$\alpha = 0.90$
−5	0.67734	0.67734	3.1669E − 7	0.67666	6.79934E − 4	0.677341	0.677341
−4	0.90061	0.90061	1.2556E − 6	0.89926	1.34472E − 3	0.900613	0.900613
−3	1.41741	1.41742	9.7011E − 6	1.41369	3.72426E − 3	1.417429	1.417430
−2	2.92872	2.92893	2.1070E − 4	2.91122	1.75083E − 2	2.928956	2.928974
−1	11.1388	11.1877	4.8900E − 2	10.8349	3.03958E − 1	11.19221	11.19684
1	11.1388	11.1877	4.8900E − 2	10.8349	3.03958E − 1	11.19221	11.19684
2	2.92872	2.92893	2.1070E − 4	2.91122	1.75083E − 2	2.928956	2.928974
3	1.41741	1.41742	9.7011E − 6	1.41369	3.72426E − 3	1.417429	1.417430
4	0.90061	0.90061	1.2556E − 6	0.89926	1.34472E − 3	0.900613	0.900613
5	0.67734	0.67734	3.1669E − 7	0.67666	6.79934E − 4	0.677341	0.677341

Table 5: Comparison of q-HATM for (case 5) when t = 0.001, a = −1, b = 1 and c = 1

x	$\lvert v_{Exact} \rvert$	$\lvert v_{\text{HATM}} \rvert$	E_1	$\alpha = 0.95$	$\alpha = 0.90$
1	1.16938	1.16511	4.2665E − 3	1.17578	1.17983
2	−1.29992	−1.30023	3.0801E − 4	−1.29935	−1.29902
3	0.313338	0.312526	8.1192E − 4	0.31478	0.31563
4	0.782071	0.782782	7.1101E − 4	0.78082	0.78008
5	−0.923472	−0.923069	4.0285E − 4	−0.92417	−0.92459
6	0.004397	0.003353	1.0441E − 3	0.00621	0.00730
7	0.909124	0.909568	4.4343E − 4	0.90835	0.90789
8	−0.760165	−0.759484	6.8133E − 4	−0.76135	−0.76206
9	−0.275279	−0.276289	1.0093E − 3	−0.27352	−0.27247
10	0.988802	0.988959	1.5752E − 4	0.98852	0.98836

Figs. 3–8 continue to illustrate cases 2 through 4, where the q-HATM is applied to solve different periodic and hyperperiodic solutions of the DNLS. For each case, both the exact and q-HATM approximations are plotted. The close alignment of the curves, particularly in Figs. 3a, 5a and 7a, reflects the ability of q-HATM to replicate the exact wave propagation dynamics with high precision. The error plots (e.g., Fig. 9) further confirm the accuracy, with q-HATM showing superior performance when compared to the homotopy perturbation method (HAM) in reducing error margins.

Figs. 9 and 10 comparative plots between q-HATM and HAM demonstrate the distinct advantage of q-HATM in producing smaller error margins. Fig. 9a,b shows the absolute difference between the q-HATM and exact solutions for cases 1 and 2, respectively, where q-HATM consistently outperforms HAM, particularly in capturing the peak and trough behavior of the wave functions. Similarly, Fig. 10a,b extends this comparison to cases 3 and 4, reaffirming the greater convergence efficiency of q-HATM across a broader range of fractional orders.

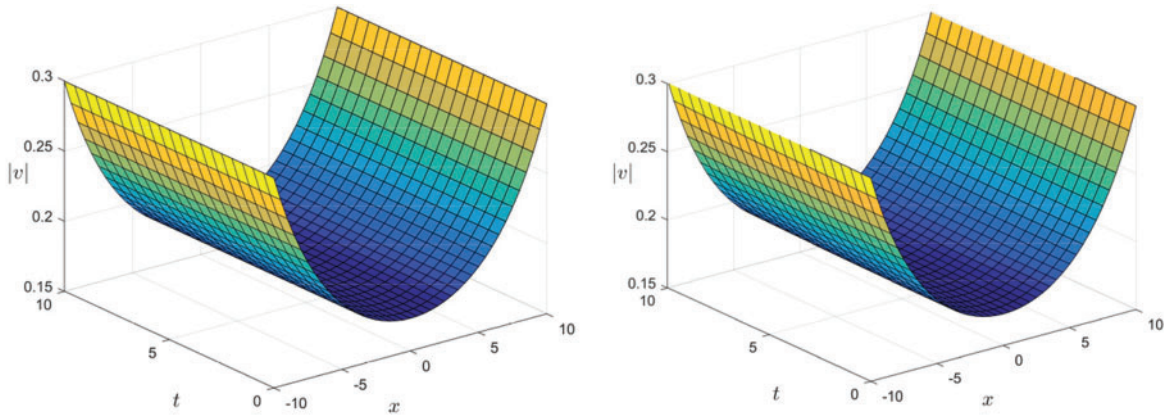

(a) Exact solution of $v(x,t)$. (b) Analytical solution of $v(x,t)$.

Figure 1: 3rd order q-HATM approximate solution $v(x, t)$ for (case 1) at $\lambda = -1, \alpha = 1, n-1$, a $= -1$, b $= 10$, and c $= 1$

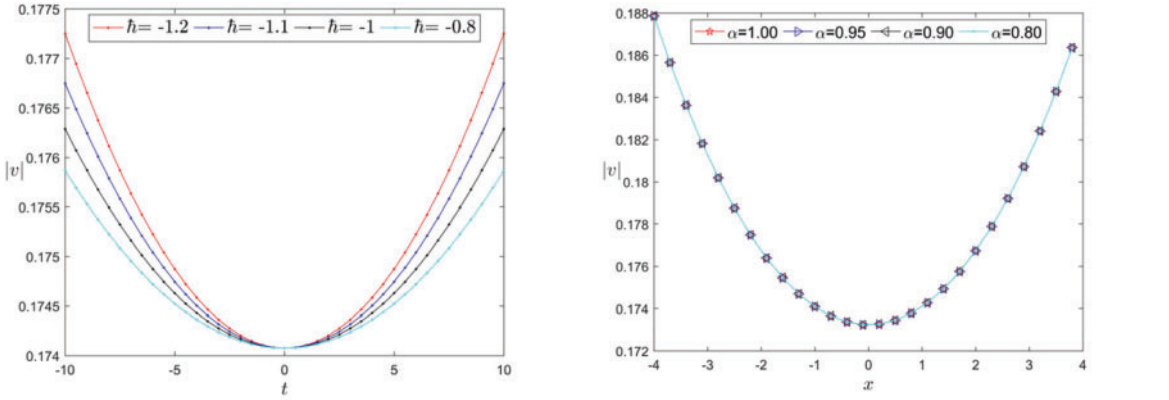

(a) λ−curve at $x = 1$, and $\alpha = 1$. (b) α−curve for different values of α at $\lambda = -1$, and $t = 10$.

Figure 2: Plot of λ-curve and plot of α-curve for (case 1) at $n = 1$, a $= -1$, b $= 10$, and c $= 1$

The figures collectively demonstrate that q-HATM is a robust and flexible method for solving fractional nonlinear systems. It not only provides accurate solutions for the DNLS but also allows for effective control over convergence through the auxiliary parameter λ, which is visually corroborated by the λ- and α-curves across different cases.

From the comparison, the q-HATM produces solutions that are significantly closer to the exact results compared to those obtained using HPM. The q-HATM not only achieves smaller error margins but also converges faster, especially for fractional orders, where traditional methods face limitations.

Our results show that q-HATM is able to handle the fractional-order derivatives and higher-order nonlinearities present in the DNLS more effectively than other methods. This study presents novel solutions that have not been reported in previous literature, particularly in the context of the fractional fourth-order cubic DNLS. Furthermore, the flexibility and control over the solution series convergence offers a practical tool for real-world applications, such as in optical fiber systems, plasma physics, and quantum mechanics, where precision in modeling wave propagation is critical.

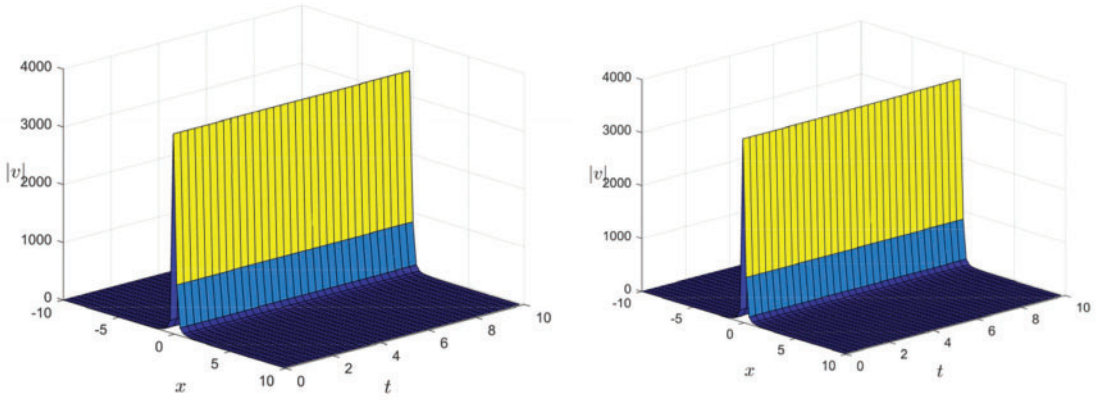

(a) Exact solution of $v(x,t)$. (b) Analytical solution of $v(x,t)$.

Figure 3: 3rd order q-HATM approximate solution $v(x,t)$ for (case 2) at $\lambda = -0.1$, $\alpha = 1$, $n = 1$, a $= -1$, b $= 10$, and c $= 1$

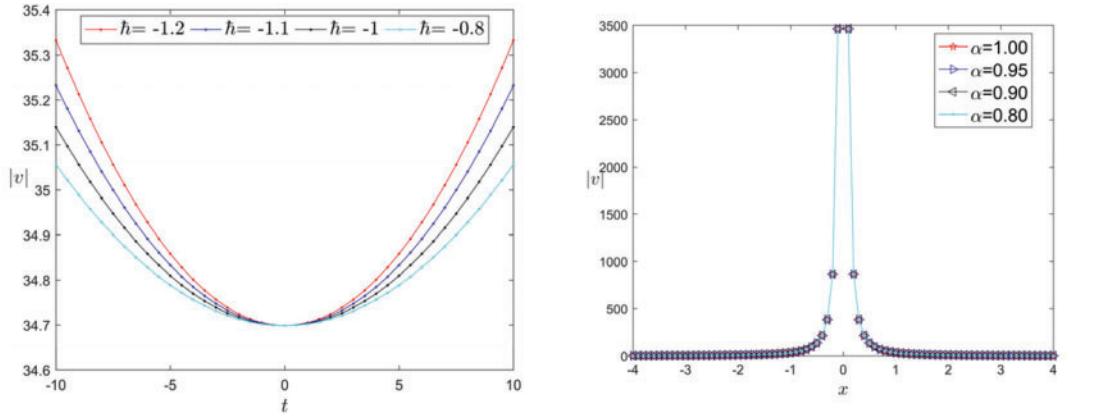

(a) λ−curve at $x = 1$, and $\alpha = 1$. (b) α−curve for different values of α at λ = −1, and t = 200.

Figure 4: Plot of λ-curve and plot of α-curve for (case 2) at $n = 1$, a $= -1$, b $= 10$, and c $= 1$

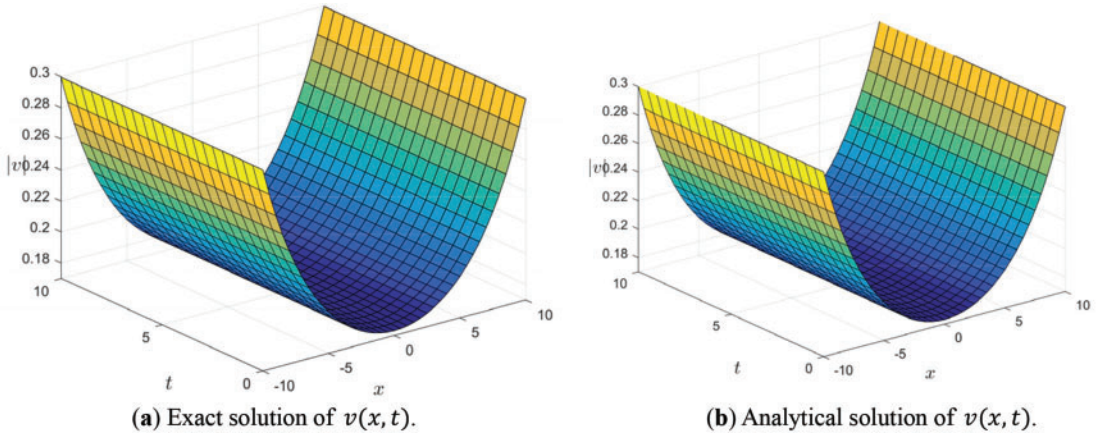

(a) Exact solution of $v(x,t)$. (b) Analytical solution of $v(x,t)$.

Figure 5: 3rd order q-HATM approximate solution $v(x,t)$ for (case 3) at $\lambda = -0.1$, $\alpha = 1$, $n = 1$, a $= 1$, b $= 10$, and c $= 1$

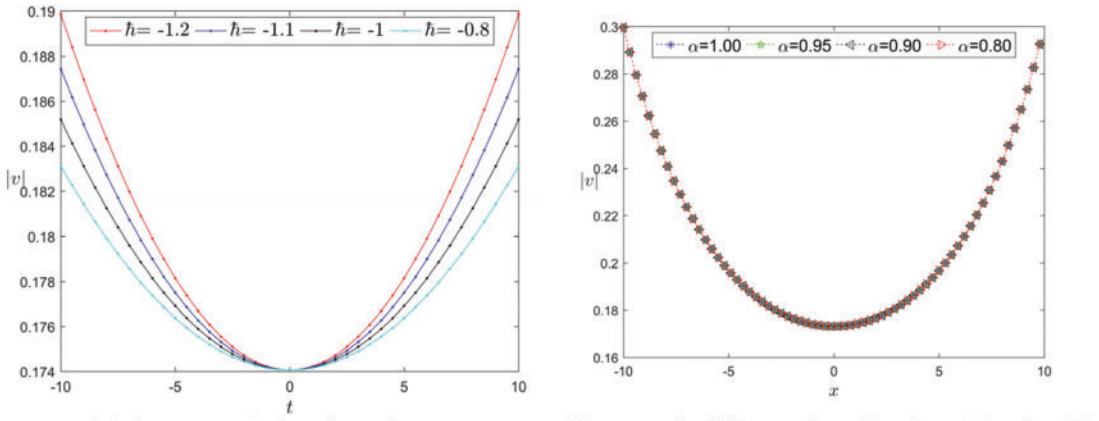

(a) λ−curve at $x = 1$, and $\alpha = 1$. (b) α-curve for different values of α at λ = −0.1, and t = 50.

Figure 6: Plot of λ-curve and plot of α-curve for (case 3) at $n = 1$, a = 1, b = 10, and c = 1

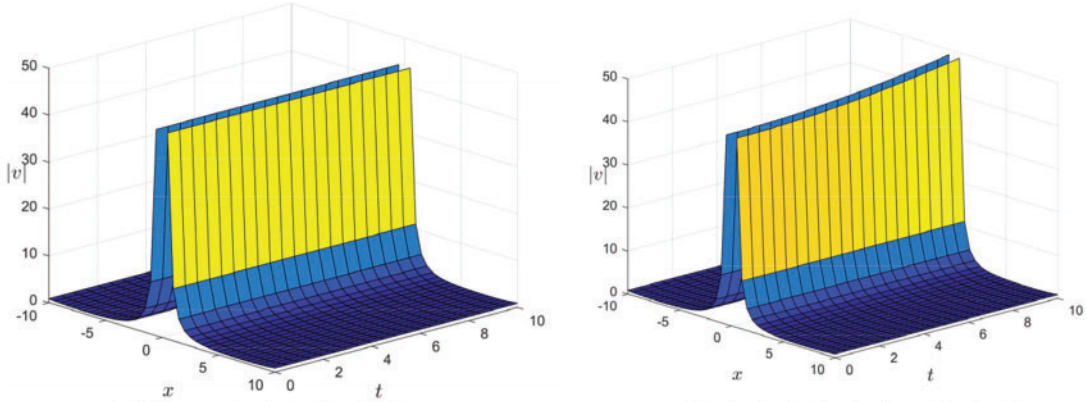

(a) Exact solution of $v(x, t)$. (b) Analytical solution of $v(x, t)$.

Figure 7: 3rd order q-HATM approximate solution $v(x, t)$ for (case 4) at $\lambda = -0.001$, $\alpha = 1$, $n = 1$, a = 1, b = 1, and c = 1

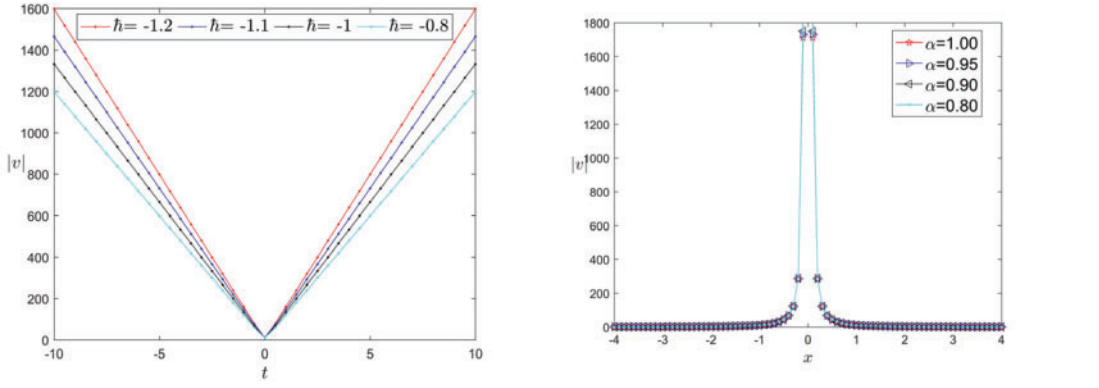

(a) λ−curve at $x = 1$, and $\alpha = 1$. (b) α-curve for different values of α at λ = −0.001, and t = 200.

Figure 8: Plot of λ-curve and plot of α-curve for (case 4) at $n = 1$, a = 1, b = 1, and c = 1

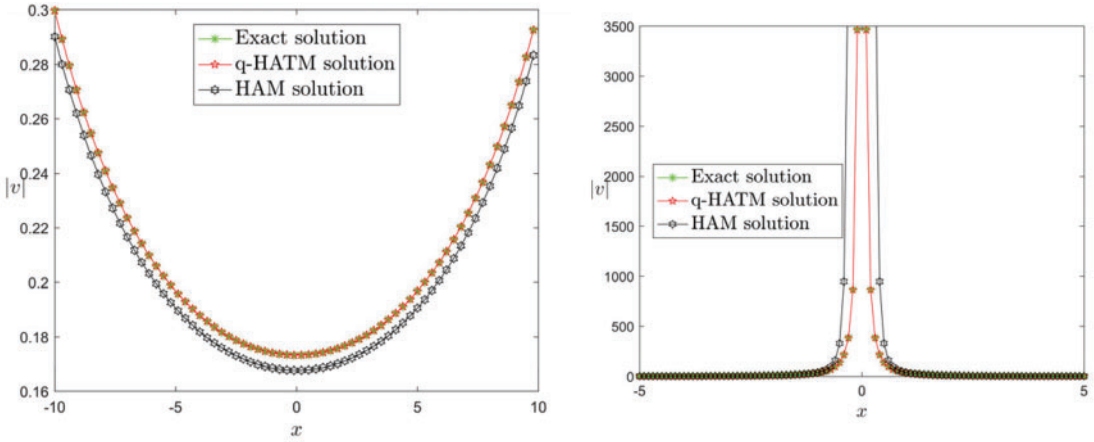

(a) Comparison for (case 1) at $\lambda = -1$. **(b)** Comparison for (case 2) at $\lambda = -0.1$.

Figure 9: Comparison between exact results, q-HATM and HAM at $\alpha = 1$, a $= -1$, b $= 10$, c $= 1$, and t $= 1$

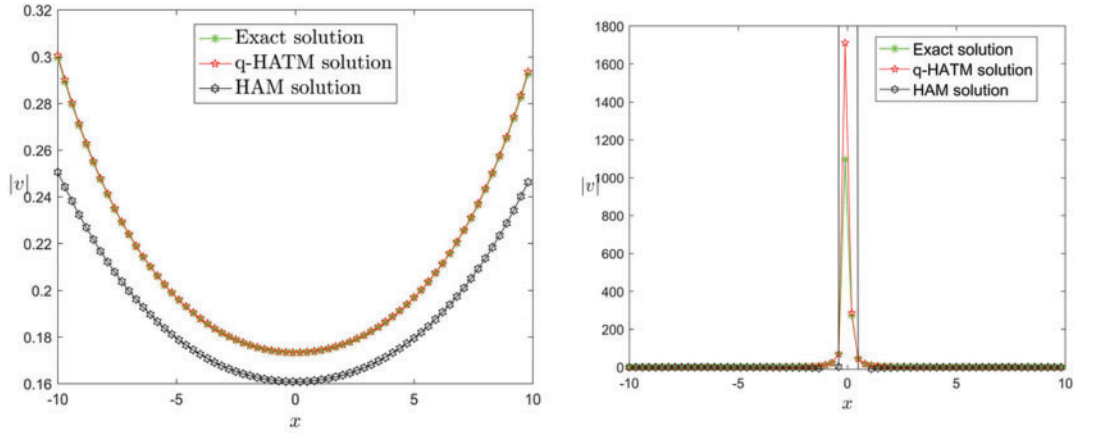

(a) Comparison for (case 3) at $\lambda = -0.1$, and b $= 10$. **(b)** Comparison for (case 4) at $\lambda = -0.001$, $\alpha = 1$, and b $= 1$.

Figure 10: Comparison between exact results, q-HATM and HAM at $\alpha = 1$, a $= -1$, b $= 10$, c $= 1$, and t $= 1$

6 Conclusion

In this paper, we presented a novel application of the q-HATM to solve the fractional fourth-order dispersive cubic nonlinear Schrödinger equation (DNLS). This study demonstrated the usefulness and robustness of the q-HATM in providing approximate solutions for complex fractional systems, which are of great importance in quantum mechanics, plasma physics, and nonlinear optics. The key contribution of this study is the application of q-HATM to fractional DNLS, a problem that has not been fully explored in prior research. The q-HATM offers several advantages over traditional methods by allowing flexible control over convergence and providing highly accurate solutions, as confirmed by comparisons with exact results. Additionally, the detailed convergence analysis ensures the reliability of the technique for solving fractional-order differential equations with higher-order dispersion. The outcomes presented in this paper are not only theoretically considerable but also highly

applicable to real-world systems, such as soliton propagation in optical fibers and wave behavior in plasma environments. This work provides a practical tool for researchers in these fields, advancing the understanding and solution of fractional nonlinear systems. These applications further emphasize the importance of fractional calculus in capturing the complexities of wave propagation, where hereditary effects and higher-order dispersion are pivotal. Fractional models provide a more comprehensive framework compared to classical models, particularly in addressing the challenges posed by ultra-fast optical pulses and quantum systems.

Acknowledgement: Not applicable.

Funding Statement: Princess Nourah bint Abdulrahman University Researchers Supporting Project number (PNURSP2025R518), Princess Nourah bint Abdulrahman University, Riyadh, Saudi Arabia.

Author Contributions: The authors confirm their contribution to the paper as follows: study conception and design: Ahmed Hagag; data collection: Anas Arafa and Zuhur Alqahtani; analysis and interpretation of results: Ahmed Hagag; draft manuscript preparation: Anas Arafa and Zuhur Alqahtani. All authors reviewed the results and approved the final version of the manuscript.

Availability of Data and Materials: Not applicable.

Ethics Approval: Not applicable.

Conflicts of Interest: The authors declare no conflicts of interest to report regarding the present study.

References

1. Az-Zo'bi E, Al-Amb MO, Yildirim A, Alzoubi WA. Revised reduced differential transform method using Adomian's polynomials with convergence analysis. Math Eng Sci Aerosp. 2020;11(4):827.
2. Rysak A, Gregorczyk M. Differential transform method as an effective tool for investigating fractional dynamical systems. Appl Sci. 2021;11(15):6955. doi:10.3390/app11156955.
3. Jazar RN. Perturbation methods in science and engineering. New York, NY, USA: Springer; 2021.
4. He JH, El-Dib YO. Homotopy perturbation method for Fangzhu oscillator. J Math Chem. 2020;58(10):2245–53. doi:10.1007/s10910-020-01167-6.
5. Alqahtani Z, Hagag AE. A fractional numerical study on a plant disease model with replanting and preventive treatment. Métodos Numéricos Para Cálculo Y Diseño En Ing Rev Int. 2023;39(3):1–21. doi:10.23967/j.rimni.2023.07.001.
6. Dawood L, Hamoud A, Mohammed N. Laplace discrete decomposition method for solving nonlinear Volterra-Fredholm integrodifferential equations. J Math Comput Sci. 2020;21(2):158–63. doi:10.22436/jmcs.021.02.07.
7. Beghami W, Maayah B, Bushnaq S, Abu Arqub O. The Laplace optimized decomposition method for solving systems of partial differential equations of fractional order. Int J Appl Comput Math. 2022;8(2):52. doi:10.1007/s40819-022-01256-x.
8. He JH, Latifizadeh H. A general numerical algorithm for nonlinear differential equations by the variational iteration method. Int J Numer Methods Heat Fluid Flow. 2020;30(11):4797–810. doi:10.1108/HFF-01-2020-0029.
9. Elboree MK. Soliton solutions for some nonlinear partial differential equations in mathematical physics using He's variational method. Int J Nonlinear Sci Numer Simul. 2020;21(2):147–58. doi:10.1515/ijnsns-2018-0188.

10. Mustafa JI. The generalization of integral transforms combined with He's polynomial. Eur J Pure Appl Math. 2023;16(2):1024–46. doi:10.29020/nybg.ejpam.v16i2.4747.
11. Nadeem M, He JH. He-Laplace variational iteration method for solving the nonlinear equations arising in chemical kinetics and population dynamics. J Math Chem. 2021;59(5):1234–45. doi:10.1007/s10910-021-01236-4.
12. Alotaibi M, Rizk D, Al-Hanaya A, Hagag A. Reliable iterative techniques for solving the KS equation arising in fluid flow. Métodos Numéricos Para Cálculo Y Diseño En Ing Rev Int. 2024;40(1):1–15.
13. Al-Hanaya A, Alotaibi M, Shqair M, Hagag AE. MHD effects on Casson fluid flow squeezing between parallel plates. AIMS Math. 2023;8(12):29440–52. doi:10.3934/math.20231507.
14. Almuneef A, Hagag AE. Approximate solution of the fractional differential equation via the natural decomposition method. Métodos Numéricos Para Cálculo Y Diseño En Ing Rev Int. 2023;39(4):1–15. doi:10.23967/j.rimni.2023.10.008.
15. El-Sayed AM, Arafa A, Hagag A. Mathematical model for the novel coronavirus (2019-nCOV) with clinical data using fractional operator. Numer Methods Partial Differ Equ. 2023;39(2):1008–29. doi:10.1002/num.22915.
16. El-Nabulsi RA, Anukool W. Higher-order nonlinear dynamical systems and invariant lagrangians on a lie group: the case of nonlocal hunter-saxton type peakons. Qual Theory Dyn Syst. 2024;23(4):161. doi:10.1007/s12346-024-01018-8.
17. El-Nabulsi RA. Emergence of lump-like solitonic waves in Heimburg-Jackson biomembranes and nerves fractal model. J R Soc Interface. 2022;19(188):20220079. doi:10.1098/rsif.2022.0079.
18. Gondal MA, Khan M, Hussain I. An efficient numerical method for solving linear and nonlinear partial differential equations by combining homotopy analysis and transform method. World Appl Sci J. 2011;14(12):1786–91.
19. Arafa AA, Hagag AMS. A different approach for study some fractional evolution equations. Anal Math Phys. 2021;11(4):162. doi:10.1007/s13324-021-00592-3.
20. Alqahtani Z, Hagag AE. A new semi-analytical solution of compound KdV-Burgers equation of fractional order. Métodos Numéricos Para Cálculo Y Diseño En Ing Rev Int. 2023;39(4):1–16. doi:10.23967/j.rimni.2023.10.003.
21. Khan M, Gondal MA, Hussain I, Vanani SK. A new comparative study between homotopy analysis transform method and homotopy perturbation transform method on a semi infinite domain. Math Comput Model. 2012;55(3–4):1143–50. doi:10.1016/j.mcm.2011.09.038.
22. Odibat Z, Momani S. A generalized differential transform method for linear partial differential equations of fractional order. Appl Math Lett. 2008;21(2):194–9. doi:10.1016/j.aml.2007.02.022.
23. Zhang R, Bilige S, Chaolu T. Fractal solitons, arbitrary function solutions, exact periodic wave and breathers for a nonlinear partial differential equation by using bilinear neural network method. J Syst Sci Complex. 2021;34(1):122–39. doi:10.1007/s11424-020-9392-5.
24. Babin A, Figotin A. Nonlinear photonic crystals: IV. Nonlinear Schrödinger equation regime. Waves Random Complex Media. 2005;15(2):145–228. doi:10.1080/17455030500196929.
25. Sultan AM, Lu D, Arshad M, Rehman HU, Saleem MS. Soliton solutions of higher order dispersive cubic-quintic nonlinear Schrödinger equation and its applications. Chin J Phys. 2020;67(10):405–13. doi:10.1016/j.cjph.2019.10.003.
26. Ohkuma K, Ichikawa YH, Abe Y. Soliton propagation along optical fibers. Opt Lett. 1987;12(7):516–8. doi:10.1364/OL.12.000516.
27. Mjølhus E. Nonlinear Alfvén waves and the DNLS equation: oblique aspects. Phys Scr. 1989;40(2):227. doi:10.1088/0031-8949/40/2/013.
28. Daniel M, Veerakumar V. Propagation of electromagnetic soliton in antiferromagnetic medium. Phys Lett A. 2002;302(2–3):77–86. doi:10.1016/S0375-9601(02)01113-1.

29. Liu SD, Fu ZT, Liu SK, Wang ZG. Stationary periodic solutions and asymptotic series solutions to nonlinear evolution equations. Chin J Phys. 2004;42(2):127–34.
30. Pang XF. The properties of the solutions of nonlinear Schrödinger equation with center potential. Int J Nonlinear Sci Numer Simul. 2014;15(3–4):215–9. doi:10.1515/ijnsns-2012-0159.
31. Ablowitz MJ, Segur H. Solitons and the inverse scattering transform. Philadelphia, PA, USA: Society for Industrial and Applied Mathematics; 1981.
32. Chabchoub A, Grimshaw RH. The hydrodynamic nonlinear Schrödinger equation: space and time. Fluids. 2016;1(3):23. doi:10.3390/fluids1030023.
33. Chabchoub A, Kibler B, Finot C, Millot G, Onorato M, Dudley JM, et al. The nonlinear Schrödinger equation and the propagation of weakly nonlinear waves in optical fibers and on the water surface. Ann Phys. 2015;361:490–500. doi:10.1016/j.aop.2015.07.003.
34. Kai Y, Yin Z. On the Gaussian traveling wave solution to a special kind of Schrödinger equation with logarithmic nonlinearity. Mod Phys Lett B. 2022;36(2):2150543. doi:10.1142/S0217984921505436.
35. Williams F, Tsitoura F, Horikis TP, Kevrekidis PG. Solitary waves in the resonant nonlinear Schrödinger equation: stability and dynamical properties. Phys Lett A. 2020;384(22):126441. doi:10.1016/j.physleta.2020.126441.
36. Zhu C, Al-Dossari M, Rezapour S, Alsallami SAM, Gunay B. Bifurcations, chaotic behavior, and optical solutions for the complex Ginzburg-Landau equation. Results Phys. 2024;59(11):107601. doi:10.1016/j.rinp.2024.107601.
37. Kai Y, Chen S, Zhang K, Yin Z. Exact solutions and dynamic properties of a nonlinear fourth-order time-fractional partial differential equation. In: Waves random complex media. UK: Taylor & Francis Group; 2022. p. 1–12.
38. Podlubny I. Fractional differential equations: an introduction to fractional derivatives, fractional differential equations, to methods of their solution and some of their applications. Cambridge, MA, USA: Academic Press; 1998.
39. Gorenflo R, Mainardi F. Fractional calculus: integral and differential equations of fractional order. Berlin/Heidelberg, Germany: Springer; 1997. p. 223–76.
40. Wazwaz AM. Exact solutions for the fourth order nonlinear Schrodinger equations with cubic and power law nonlinearities. Math Comput Model. 2006;43(7–8):802–8. doi:10.1016/j.mcm.2005.08.010.
41. Al Qurashi MM, Yusuf A, Aliyu AI, Inc M. Optical and other solitons for the fourth-order dispersive nonlinear Schrödinger equation with dual-power law nonlinearity. Superlattices Microstruct. 2017;105(8):183–97. doi:10.1016/j.spmi.2017.03.022.